A Cryosphere-Hydrology Observation System in a Small Alpine Watershed in the Qilian Mountains of China and Its Meteorological Gradient

Authors: Chen, R. S., Song, Y. X., Kang, E. S., Han, C. T., Liu, J. F., et al.

Source: Arctic, Antarctic, and Alpine Research, 46(2) : 505-523

Published By: Institute of Arctic and Alpine Research (INSTAAR), University of Colorado

URL: https://doi.org/10.1657/1938-4246-46.2.505

Arctic, Antarctic, and Alpine Research, Vol. 46, No. 2, 2014, pp. 505–523

A Cryosphere-Hydrology Observation System in a Small Alpine Watershed in the Qilian Mountains of China and Its Meteorological Gradient

R. S. Chen†*
*Y. X. Song**
*E. S. Kang**
*C. T. Han**
*J. F. Liu**
*Y. Yang**
W. W. Qing and*
*Z. W. Liu**

*Qilian Alpine Ecology and Hydrology Research Station, Key Laboratory of Inland River Ecohydrology, Cold and Arid Regions Environmental and Engineering Research Institute, Chinese Academy of Sciences, 320 Donggang West Road, Lanzhou 730000, China
†Corresponding author: crs2008@lzb.ac.cn

Abstract

The unavailability of sufficient data at higher elevations causes many uncertainties in research on cold regions. This study considers a cryosphere-hydrology observation system established in 2008 at the Hulu small alpine watershed in the Qilian Mountains of Northwest China. The altitudinal gradient of weather factors is analyzed using data from the Hulu watershed and routine stations located in the Heihe upstream. The data presented here provide the following knowledge of mountain meteorology at elevations from 3367 m to 4166 m/4248 m in the Qilian Mountains: (1) the yearly precipitation–altitude relationship is linear in regions below 4248 m in the Heihe upstream, where the precipitation gradient increased marginally from 1960 to 2011; (2) the yearly air temperature lapse rate (TLR) is weaker at higher elevations (>3000 m), and the seasonal TLR became more divergent between winter and summer half-years from 1960 to 2011 (yearly mean 5.6 °C km^{-1}); (3) in the Hulu watershed, the LRs of water vapor pressure and absolute humidity are higher in warm seasons with yearly means of 1.1 hpa km^{-1} and 0.84 g m^{-3} km^{-1}, respectively, and the maximum relative humidity value is found at elevations between 3500 and 3700 m in the Heihe upstream; (4) the long-term existence of snow increases the albedo to yearly means of 0.22, 0.30, 0.35, and 0.27 in areas of grassland, meadow, marshy meadow, and alpine desert in the Hulu watershed, respectively. The relationship between monthly net radiation and soil surface temperature (Ts) is linear, and the mean Ts LR was about 7.5 °C km^{-1} from July 2009 to September 2011.

DOI: http://dx.doi.org/10.1657/1938-4246-46.2.505

Introduction

Cold regions are a major research frontier for atmospheric and hydrologic sciences (Woo, 2008). Harsh climates, isolation, and the high cost of research have often discouraged field investigations, and most research to date has been limited in scope, focusing on particular aspects of the environment such as the climate, hydrology, vegetation, or landforms (Nuttall and Callaghan, 2000), whereas many aspects of the natural environment are interconnected (Woo, 2008). Cold regions in China accounting for 43.5% of the country's land area together constitute the headstreams of most large rivers in Asia (Chen et al., 2006). A shortage of data has also restricted research on the cryosphere and aspects of alpine hydrology and ecology that are highly sensitive to climate change in high altitude cold regions in China (about 298.6×10^4 km^2). For example, Anduo Station, the highest of China's routine meteorological stations, is located in the flat area of the Tibetan Plateau at an elevation of 4800 m, while the mean altitude of the Tibetan Plateau is about 4325 m, and many of the surrounding mountains are much higher than Anduo Station. This means there is little knowledge from point to regional scale on many aspects of the natural environment in China's high altitude cold regions.

The Qilian Mountains lie in the northeastern part of the Tibetan Plateau, rising to altitudes of between 2000 m and 5800 m and spanning 800 km from west to east, and their vegetation clearly follows a vertical zonal distribution. They represent an important ecological barrier in China and are also the source region for three large arid inland river basins in the Hexi Corridor (from east to west, the Shiyang, Heihe, and Shule river basins, respectively, covering a combined area of about 300,000 km^2). Most of the mid- and downstream areas in these inland river basins are covered by desert, and the runoff from the Qilian Mountains is the only water resource that can be allocated for human consumption (Kang et al., 2005). Therefore, ecology and hydrology research in the Qilian Mountains may be important for both runoff estimation and local ecology retention. However, data limitations have also frustrated progress in this research field. Taking the scarcity of climatic data as an example, there are only a few routine meteorological stations in the Heihe mountainous watershed covering an area of 27,000 km^2, among which the highest (Tuole Station) is located at an altitude of about 3367 m, significantly lower than the average elevation of the watershed (about 3575 m).

Although climate, ecology, the cryosphere, and hydrology are interconnected in cold regions, most research conducted in China's cold regions to date has been limited in scope in a similar manner to the Arctic study presented by Nuttall and Callaghan (2000). Due to the shortage of synchronous measured data on the climate-cryosphere-ecology-hydrology system in watersheds in China's high altitude cold regions, we still lack a clear understanding of water and heat transfer processes in the frozen soil-vegetation-atmosphere transfer system (SVAT system) on different underlying surfaces, and of the functions of the cryosphere and altitudinal vegetation zonation (Kang et al., 2008). Given this situation, hydrological simulation and other aspects of research have a large degree of uncertainty. The authors therefore established a cryosphere-hydrology observation system including vegetation in a small alpine watershed in Heihe in the Qilian Mountains, northwestern China, in 2008. This observation system emphasizes

1523-0430/18 $7.00

alpine hydrology to some extent. This paper gives an overview of the small watershed established by the authors and its meteorological gradient at altitude; the other results will be reported later.

Observation Network in the Small Watershed

The small alpine watershed, the Hulu watershed, lies from 99°49′ to 99°54′ in longitude and from 38°12′ to 38°17′ in latitude, with an altitude range of approximately 2960 to 4800 m and a drainage area of about 23.1 km^2 (Fig. 1, part a). The Hulu watershed was chosen as the venue for long-term field experiments for two main reasons. First, the area covers about 92% of the altitude range from about 2960 to 4800 m in the upstream section of the Heihe mainstream basin (10,009 km^2, 1674 to ~5110 m; Chen et al., 2008); that is, the Hulu watershed is highly representative of the Heihe upstream basin in terms of altitude. Second, nearly all typical underlying surfaces in high cold regions can be found there, such as glacier, snow, permafrost, and seasonal frozen soil, alpine desert, marshy meadow, alpine meadow, alpine shrubs, forest, and alpine grasslands (Fig. 1, part b). The field experiments started in August 2008 and are still being refined.

In spatial terms, the field experiments could be classified into four types by scale: point, slope, sub-watershed, and small watershed. The point scale experiments are distributed over the Hulu watershed and involve many scientific subjects. Three slope scale experiments are being conducted: each involves using the runoff field to contrasting shrubs with meadow, glacier, and forest water balance fields. Two sub-watersheds with hydrological sections and meteorological variables, soil water content and temperature, and ecological quadrats, etc., were specifically chosen for alpine desert and alpine meadow, because these two underlying surfaces cover about 22% and 52% of the upstream area of the Heihe mainstream basin, respectively (Figs. 1 and 2).

By subject, the field experiments focus on the cryosphere, ecology, meteorology, and hydrology, and so on, and could be roughly classified as cryospheric hydrology. For convenience, the following paragraphs describe the experiments according to their content.

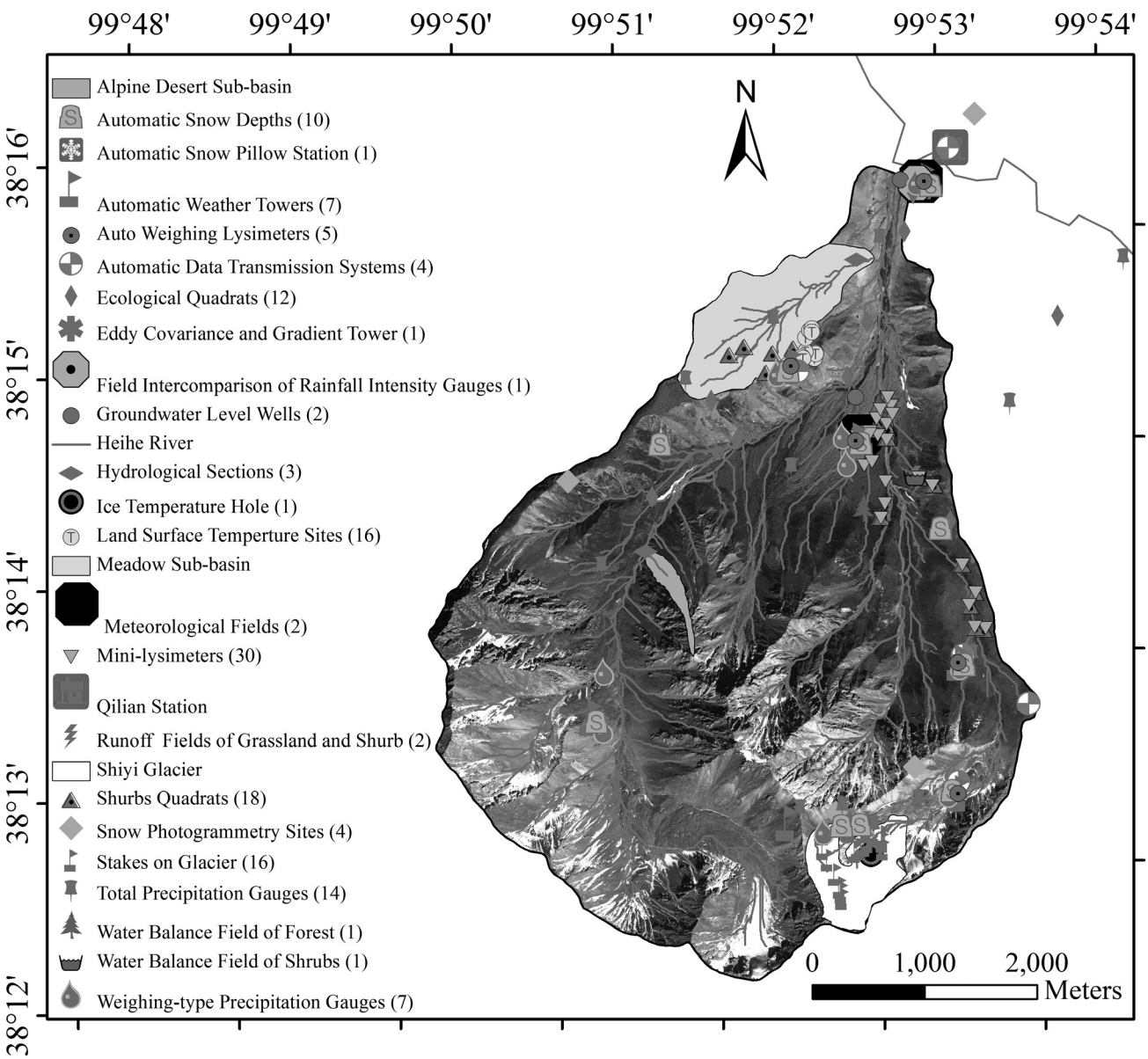

FIGURE 1. (a) Observation network.

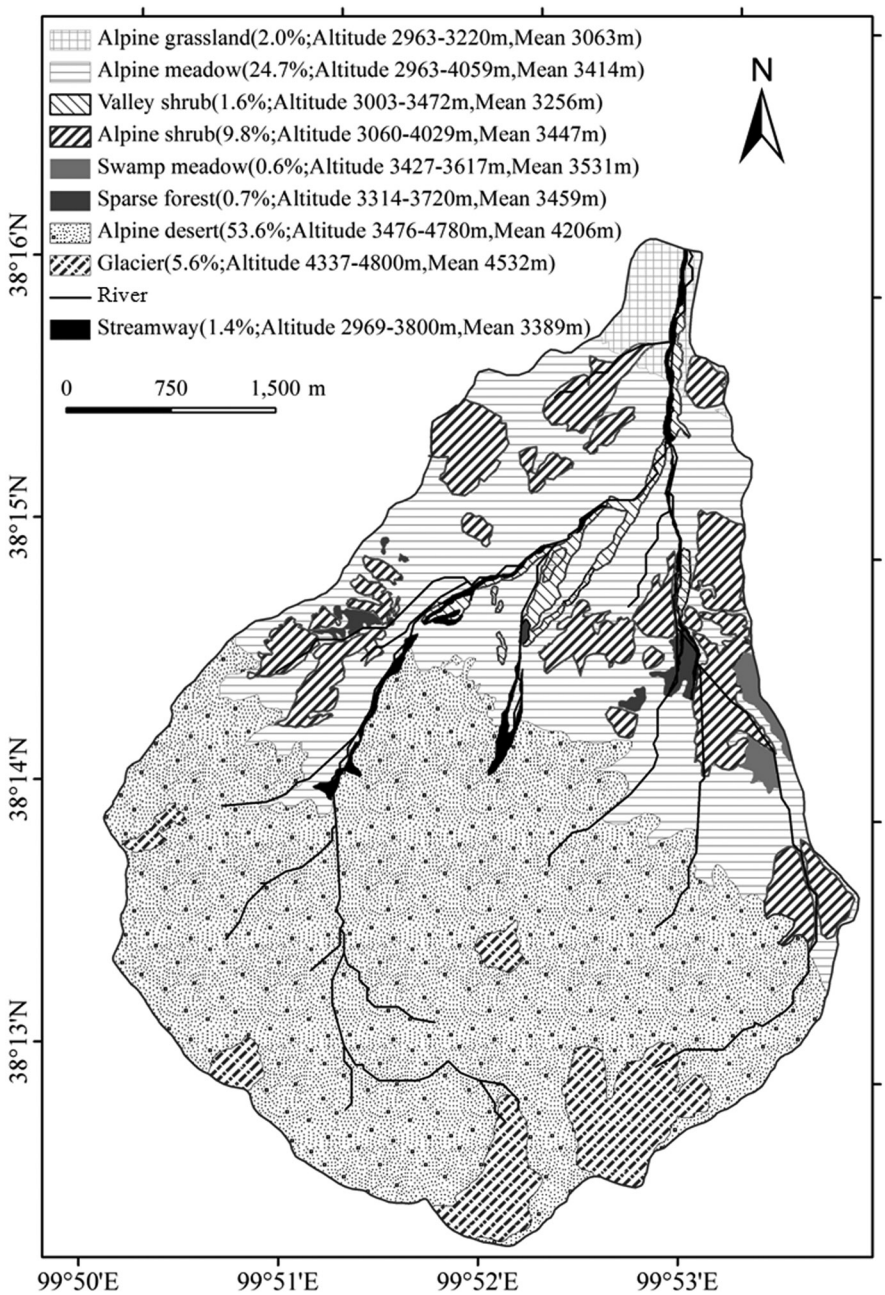

FIGURE 1 (continued). (b) Landscapes in the Hulu watershed.

METEOROLOGY

Meteorology, especially precipitation, is very limited in the alpine regions in China. The small watershed at Hulu has a total of five automatic meteorological towers (Table 1) and two meteorological parks before 2013. In October 2013, two new towers were set up (Fig. 1, part a). One of the meteorological parks was designed as a national standard field, while the other has a more straightforward design. In the standard field, at all stations other than automatic station no. 5 (Table 1), atmospheric pressure, air temperature (maximum, minimum, and routine), relative humidity, sunshine hours, evaporation, diameter (d) (d = 20 cm), soil temperature (surface and superficial layer), frozen soil depth, and weather phenomena have been observed manually since June 2009. In addition, two mini-lysimeters (d = 31.5 cm, h = 40 cm) are used to measure evapotranspiration on alpine grasslands twice a day. To reduce measurement error, readings from five rain gauges are contrasted in making rainfall and snowfall observations. One is the China standard recorder (d = 20 cm, h = 70 cm) used in all routine stations in China; the second is also the routine model, but with a windshield (Alter windshield); the third and fourth are pit gauges with different caliber sizes (d = 20 cm, area [S] = 500 cm^2; Goodison et al., 1998); and the last one is the Double-Fence International Reference (DFIR). In the simple field, a siphon rainfall recorder, an evaporating dish, one T-200B series precipitation gauge (Geonor), and four mini-lysimeters were set up in October 2011 in all stations other than automatic station no.4 (Table 1). To detect the complexities of alpine precipitation, a total

of 14 totalizers and two weighted rainfall recorders (self-made, with a one-layer wind, air temperature, and relative humidity) have also been installed over the small watershed (2960 to ~4650 m) in June 2009 and in July 2012, respectively. Now for the precipitation, there are a total of seven automatic weighted rainfall recorders, one tipping-bucket rain gauge, one siphon rainfall recorder, two China standard recorders, and 14 totalizers in the Hulu watershed. Data used here except from the totalizers are roughly calibrated by the pit gauges (A500). The more detailed calibration would wait for the DFIR data.

GLACIERS

The Hulu watershed has a total of six glaciers, the combined area of which has fallen from 1.45 km^2 in 1956 (Wang, 1981) to 1.01 km^2 in 2010 (using Global Positioning System Real Time Kinematic [RTK-GPS], 2010). Among the six glaciers, one has disappeared and one has separated into two glaciers. The largest one, Shiyi Glacier, has shrunk in area from 0.64 to 0.54 km^2 and has a glacier terminus that has risen from 4270 to 4320 m in the past 55 years (1956 to ~2010). Ground-penetrating radar data indicate the maximum depth of Shiyi Glacier was about 70 m in October 2010. Shiyi Glacier was chosen for monitoring because its type (a combination of valley glacier and hanging glacier) and area are close to those typical of the Qilian Mountains (most glaciers are hanging or valley glaciers with a mean area of about 0.33 km^2).

A total of 6 stakes and 2 totalizers were installed in Shiyi Glacier in July 2009, with 15 stakes and 1 glacier temperature bore being added in October 2010 (Fig. 1, part a). Because of the appearance of several moraines, the glacier runoff is sometimes roughly estimated by using isotopes instead of measuring it directly. A simple automatic station with a one-layer wind, air temperature, humidity, and weighted rainfall recorder is installed in the glacier in July 2012. Several charge coupled device (CCD) cameras with storage cards are also being installed to monitor matter balance according to the gauge changes in the stakes.

SNOW

Snow is monitored automatically and manually on point, line, sub-watershed, and small watershed scales. On a fixed point scale, there are four snow depth probes measured every half hour in the automatic stations (Table 1, stations no. 1–4). Snow depth is a routine measurement variable in the standard meteorological field after every event. Near the simple meteorological field, there is a special snow field (close to automatic meteorological station no. 4 shown in Table 1) including a snow pillow (3 m × 3 m), a Flowcapt sensor (3 m high), a T-200B series precipitation gauge, two snow depth probes (SR50A), an infrared land surface temperature gauge (SI-111), and soil moisture and temperature gauges.

After major snowfall, the depth, density, and water content of the snow are investigated using a snow fork (Toikka, Finland) along the two relatively fixed lines near the main branches of the Hulu watershed (see Fig. 1, part a).

On the sub-watershed and small watershed scales, terrestrial photographic methods have been used to record changes in snow area every four hours (automatically) since March 2010. One camera (Canon EOS 7D with Canon EF 50mm f/1.4 USM Lens) using time-lapse photography was installed in March 2010 and three cameras (Canon EOS 5D) were installed in July and October 2012 to reduce shading. For the terrestrial photography method, high-precision digital elevation data (DEM) are needed for calibration and blowing snow research. It comes from the telemetry data (Light Detection and Ranging, LDAR, 1 m × 1 m) in the second Hi-WATER (Li et al., 2009) experiment in August 2012.

Isotopes research specifically funded by the National Natural Sciences Foundation of China has been applied to learn more about snow flow concentration routes since 2012.

FROZEN SOIL

Permafrost (above 3700 m) and seasonal frozen soil are both found in the Hulu watershed. The permafrost area is so difficult to climb that there are no deep soil temperature bores at present. Only the active layer and seasonal frozen soil are currently monitored. Multilayer soil moisture and temperature are measured in all five automatic meteorological towers shown in Table 1. The soil profile in stations no.1–3 and 5 is about 1.6 to ~2.0 m, while in station no. 4 it is 3.0 m. In addition to these weather requirements, the five stations have been specially installed on five different underlying surfaces (see Table 1) to enable discussion of the water and heat transfer processes in the frozen soil-vegetation-atmosphere-transfer system (SVATs). Stations no. 2 and 3 lie in the permafrost area with active layer depths of 3.5 and 2.4 m, respectively. The maximum freezing depths in the regions where stations no. 1, 4, and 5 are located are about 1.3 m (sunny slope, 3382 m), 2.7 m (flat area, 3232 m), and 2.4 m (flat area, 2980 m), respectively.

Furthermore, in the two meteorological fields, the soil temperature in superficial layers (≤45cm) is measured manually. Freezing depth (<3.0 m) is also measured in the standard meteorological field. Considering the land surface temperature is measured only in flat bare soil at routine stations in China, a total of 24 recorders (TidbiT v2, Onset, USA) have been fixed at locations with different azimuth, slope, and vegetation types at similar elevations (see Fig. 1). By combining the data these recorders gather with such things as solar elevation and air temperature readings, an empirical formula on land surface temperature may be created for cryospheric sciences and other subjects.

ALPINE DESERT

Alpine desert areas with a high elevation, a cold climate, steep terrain, little vegetation cover, and a large area ratio (about one-third) should be used as the main runoff production areas in high altitude cold regions in China (Chen and Han, 2010), but little has been done to investigate them. Alpine desert occupies about 50% of the Hulu watershed, making it larger than that in the Heihe upstream basin (Fig. 1, part b, and Fig. 2). It is monitored at two sites, one being automatic station no. 3 (Table 1) and the other being a special sub-watershed (see Fig. 1, part a). At station no. 3, an automatic mini-lysimeter has been installed in August 2013 to enable better analysis of the water balance. Though the highest elevation of the small sub-watershed (0.13 km^2 in area) is only 4280 m, it is the only one with a well-controlled hydrological section (3611 m in altitude) in the Hulu watershed. In addition to the meteorological network established in the Hulu watershed, precipitation, infiltration, evaporation (monitored through an evaporating dish and six mini-lysimeters), and condensation in the alpine desert were observed at a site (3719 m) near the discharge zone of the sub-watershed from 7 June to 30 September 2009. The runoff has been measured manually since June 2009, and a CCD camera with a storage card is fixed to monitor its water level in July 2012.

TABLE 1
Information on the five automatic meteorological towers.

Station No.	Longitude	Latitude	Altitude (m)	Land use	Air temp.	Rel. humid.	Wind	Precipitation	Snow depth	Sunshine hours	Solar radiation	Soil heat flux	Land surface temp.	Soil temp.	Soil water content	Air pressure	CO_2	Start date
1	99°52.2′E	38°15.3′N	3382	Alpine meadow	2-layer (Model 43502, R. M. Young)		2-layer (WindSonic, Gill)	TRwS 500, MPS (Slovakia)	SR50A, Campbell	CSD3, Kipp & Zonen	CNR1, Kipp & Zonen	3 probes (HFP01, Campbell)	S1-111, Apogee	8-layer (109, Campbell)	8-layer (Enviro SMART Sentek)	—	—	Aug 2008
2	99°53.4′E	38°13.9′N	3711	Marshy meadow												—	—	
3	99°53.4′E	38°13.3′N	4166	Alpine desert												—	—	
4	99°52.6′E	38°14.9′N	3232	Forest, shrub meadow	4-layer, 10-m tower; same as above					—						—	EC150, Campbell	Oct 2011
5	99°52.9′E	38°16.1′N	2980	Alpine grassland	2-layer (HMP45D, Vaisala)		2-layer (Lisa/Rita, SG GmbH)	RG50, SG GmbH	—	—	CM78/ NR-Lite Kipp & Zonen			7-layer (T8. IMKO)	7-layer (TRIME-EZ, IMKO)	PTB100, Vaisala	GMM222, Vaisala	Jun 2009

ALPINE MEADOW

In addition to the point scale experiment outlined in Table 1 and Figure 1, part a, a special sub-watershed for alpine meadow has been monitored since June 2009. This sub-watershed has an area of 1.1 km^2 and ranges in altitude from 3050 to 3570 m. Automatic meteorological station no. 1 (see Table 1), three totalizers, 24 land surface temperature recorders, several ecological quadrats, nine superficial layer temperature bores, and a regular hydrological section with a HOBO water level logger (Hobo u20-001-01, Onset, U.S.A.) have been installed to facilitate discussion of the hydrological processes and ecohydrological functions of the alpine meadow. Because the water flow is low in this sub-watershed, the HOBO logger has been replaced by a CCD camera with a storage card since July 2012. An automatic mini-lysimeter was set up to observe evapotranspiration at automatic meteorological station no.1 in August 2013.

FOREST

Most of the trees in both the Hulu watershed and the Qilian Mountains are of two species (*Piceacrassifolia* and *Sabina prezewalskii*). The former tree species, found in various locations abroad, lives on shady slopes, while the latter prefers sunny slopes. *Piceacrassifolia* has been arbitrarily defined as a water conservation forest species in the past, but its water balance is still not known (Kang et al., 2008). In contrast, the limited evapotranspiration research results obtained using sapflow techniques demonstrate that *Piceacrassifolia* has very large transpiration (Chen et al., 2004). Thus, a water balance field for *Piceacrassifolia* has been in place since May 2010.

In the water balance field, out of forest precipitation comes from automatic meteorological station no. 4, a T-200B series precipitation gauge and a siphon rainfall recorder. The throughfall and stem-flow of four *Piceacrassifolia* trees are measured manually using self-made instruments. A total of four sapflow sensors (CAF, ECOMATIK) have been installed in the four trees to estimate transpiration. Two or three automatic homemade mini-lysimeters will also be set up in 2014 to measure soil evaporation in the forest.

ALPINE SHRUBS

Shrubs occupy 20% of cold regions in China. Because they often grow on meadow in high-altitude zones, shrub meadows are often broadly categorized as ecological or alpine meadow features in interpreting remote sensing data. Alpine shrubs are distributed broadly across the Hulu watershed (9.8%; Fig. 1, part b). Four main alpine shrub types (*Caraganajubata*, *Potentillafruticosa*, *Salix cupularis,* and *Hippophaerhamnoides*) have been chosen to measure throughfall and stem-flow to raise awareness of canopy interception. An eddy covariance system (EC150, Campbell, Fig. 1, part a) mounted on a 10 m tower (automatic station no. 4 shown in Table 1) has been used to observe regional evapotranspiration since October 2011. About 20 mini-lysimeters have been used to measure shrubs' evapotranspiration manually since October 2012. In addition, about 20 ecological quadrats have been investigated since May 2010 (Fig. 1, part a).

GROUNDWATER

Groundwater flow is difficult to estimate in alpine watersheds with complex terrain. Two groundwater wells, each of which has

two HOBO sensors (Onset, USA), were drilled in October 2011 (Fig. 1, part a). Isotope and hydrochemical methods have been applied since 2012.

DISCHARGE

Discharge is now measured both manually and automatically in three sections (Fig. 1, part a). One is located in the discharge zone of Hulu watershed, whereas the other two lie in alpine desert and meadow sub-watersheds. The weirs are well designed and built. Flow velocity and water level are measured manually, with readings decreasing from every two hours in June 2009 to three times per day now. Two HOBO sensors (Onset, USA) have been installed in the lenitic wells to record the water level in each section. A CCD camera with a storage card was set up to complement these sensors in June 2012 and obtain more accurate water level data.

ECOLOGY QUADRATS AND SOIL INVESTIGATION

Basic soil and vegetation data are regularly gathered in the Hulu watershed (Fig. 1, part a). Though land use data and vegetation types are respectively acquired from Advanced Land Observing Satellite (ALOS, 2.5 m) images (Fig. 1, part b) and field investigations, they are somewhat raw. Now the more detailed data are obtained from the aerial remote sensing in the second Hi-WATER (Li et al., 2009) experiment conducted in July and August 2012.

Altitudinal Gradient of Meteorological Variables and Discussion

PRECIPITATION (P)

Insufficient P data is the largest source of uncertainty for watershed hydrology in alpine regions in both China and the rest of the world. Much work has been conducted to obtain accurate regional P measurements. Lauscher (1976) used global data collected at 1300 stations to discuss the relationship between P and elevation, but only 3.3% of the stations concerned lie above 2000 m a.s.l. As more data collected and methods used in large mountain ranges have been reported (e.g., Shen, 1975; Fo, 1992; Basist et al., 1994; Lin, 1995; Johnson and Hanson, 1995; Aizen et al., 1996; Thomas, 1997; Sevruk and Nevenic, 1998; Rubel and Rudolf, 2001; Sevruk and Mieglitz, 2002; Marquínez et al., 2003; Putkonen, 2004; Ahrens, 2006; Prat and Barros, 2010; Wulf et al., 2010; Akkiraz et al., 2011; Kotlarski et al., 2012), significant advances have been made over the past few decades, leading to a greater understanding of many aspects of the basic mechanisms responsible for orographic P (Roe, 2005; Barry, 2008). However, because most of these reports still suffer from a lack of data gathered in mountainous higher regions, the accuracy of their results is still very limited (Marquínez et al., 2003; Ward et al., 2011); important issues remain unresolved (Roe, 2005); and the unsatisfactory degree of accuracy in P forecasting means an increase in the use of observational data is still necessary (Michaelides et al., 2009). The need for P observations was recently assessed by a EUMETSAT expert group (Rizzi et al., 2006). Their investigation covers meteorological applications—both numerical

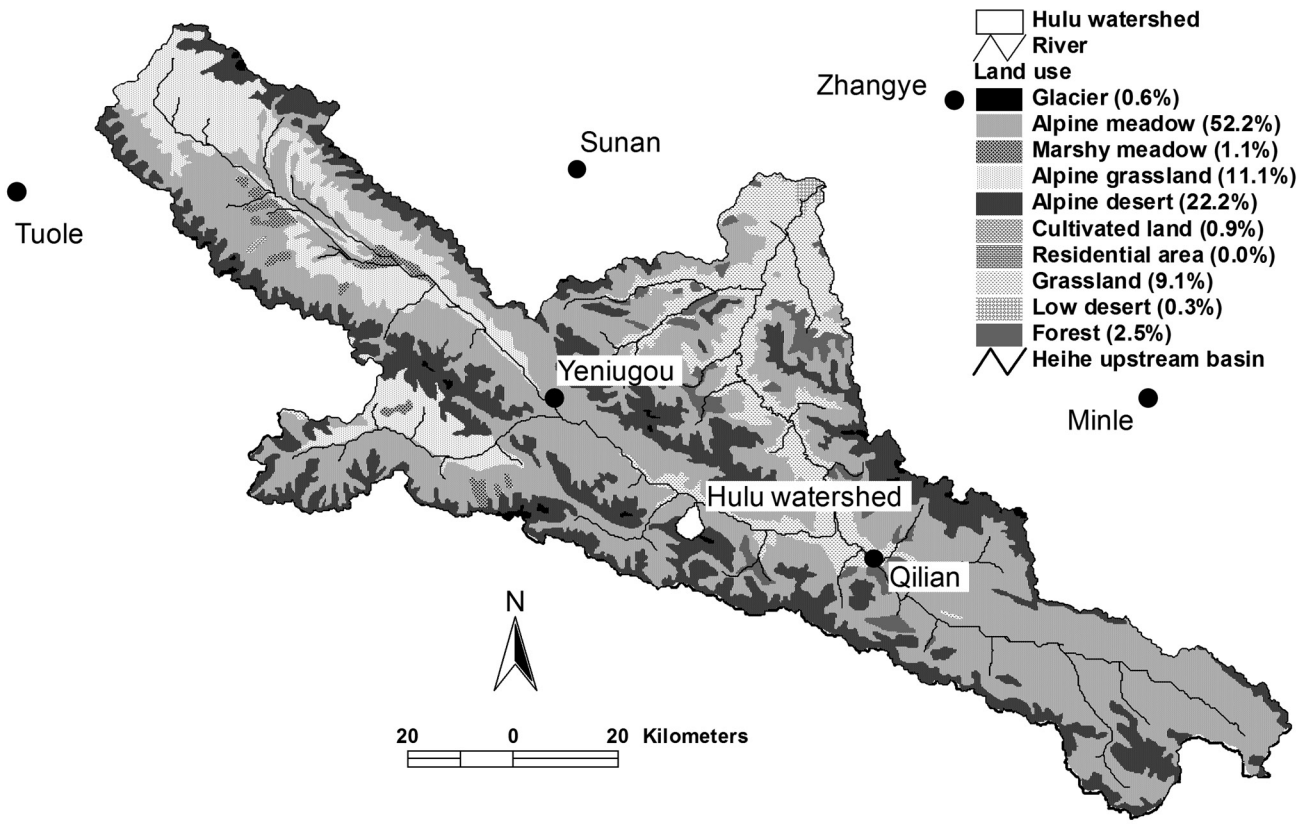

FIGURE 2. Land uses, weather stations, and position of Hulu watershed in the upstream section of the Heihe mainstream basin (10,009 km^2).

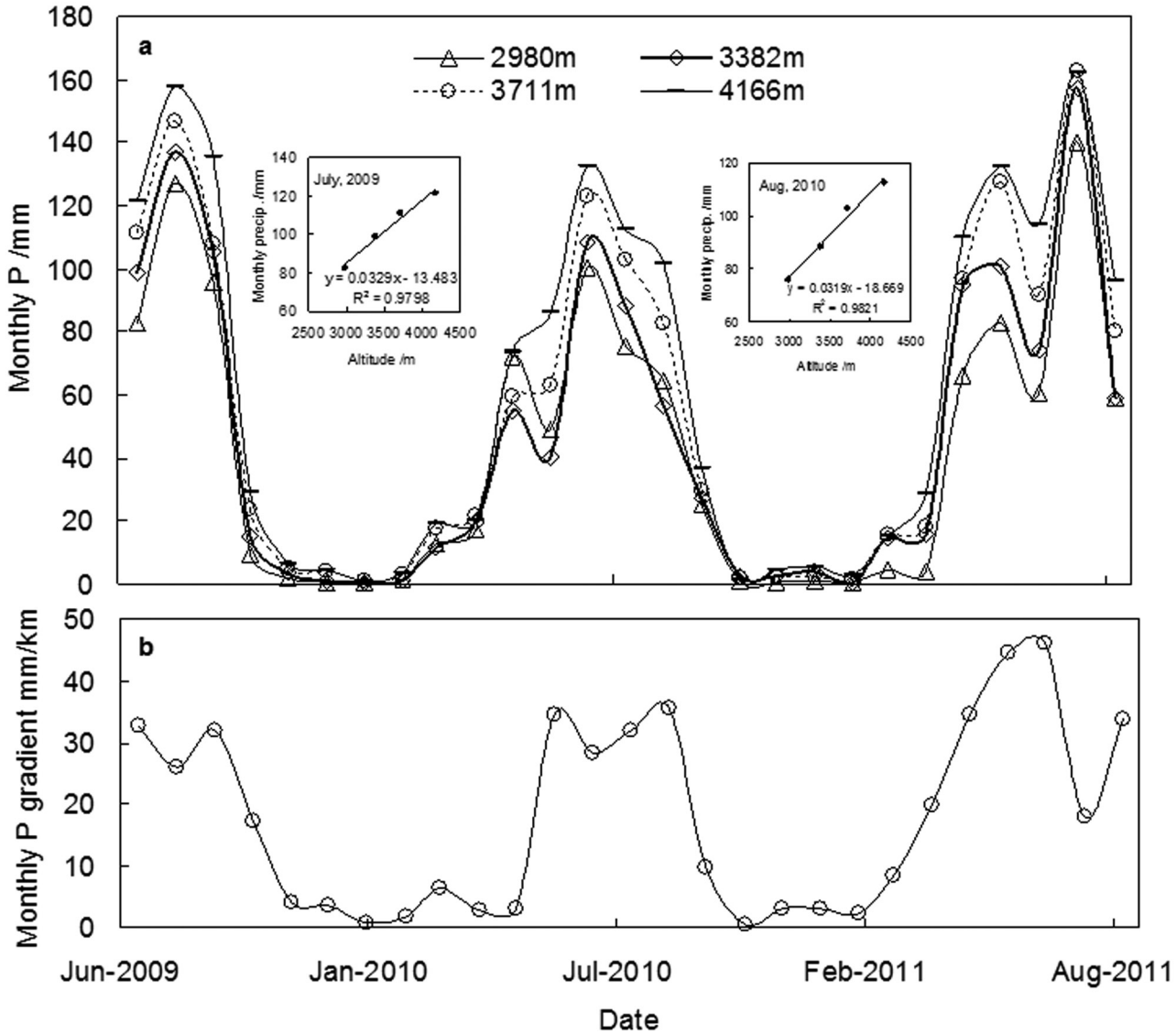

FIGURE 3. Monthly precipitation (P) at 4 sites and its altitudinal gradient from July 2009 to September 2011 in the Hulu watershed.

weather prediction (NWP) and NoWCasting (NWC)—as well as hydrology and climate, for 2020 onward. Conventional P measurements obtained from gauges, or more recently from radar, will clearly not satisfy these requirements on a global basis (Prigent, 2010), whereas P data produced from space and at ground level are still not satisfactory in complex mountains (Ward et al., 2011).

Our results show that, on a monthly scale, a P gradient is evident in the Hulu watershed (mean R^2 = 0.98, a = 0.01) other than in some months (Fig. 3), similar to the results obtained in Tien Shan (Aizen et al., 1996). Most of the exceptions occurred at the 2980 m site and the 3382 m site in winter 2009, May and November 2010, and September 2011 (Fig. 3, part a) when the precipitation was little.

The P gradient is evidently subject to seasonal differences. It is about 35 mm km^{-1} in summer, 3 mm km^{-1} in spring and autumn, and 15 mm km^{-1} in winter (Fig. 3, part b).

All the routine weather stations (Table 2; see Fig. 2) in or near the upstream watershed are used to learn more about the P

TABLE 2

Routine weather stations in or near the upstream of the Heihe main stream basin.

Stations	Zhangye	Minle	Sunan	Qilian	Yeniugou	Tuole
Longitude (E)	100°26′	100°49′	99°37′	100°15′	99°35′	98°25′
Latitude (N)	38°56′	38°27′	38°50′	38°11′	38°25′	38°48′
Altitude (m)	1482.7	2271.5	2311.7	2787.4	3320.0	3367.0

gradient in the whole upstream section of the Heihe mainstream basin where Hulu water is located. In rainy seasons, the P-altitude relationship in the upstream section of the Heihe mainstream watershed is clearly linear, with some exceptions occurring at Tuole Station (e.g., September 2009, August 2010, May and September 2011; Fig. 4), because it is far from the other stations (see Fig. 2). From altitudes of 1483 m (Zhangye Station) to 4166 m (automatic weather station no. 3 in the Hulu watershed), no visible so-called maximum P elevation zone is found on monthly scale. The relationship between P and altitude is complex in arid and cold

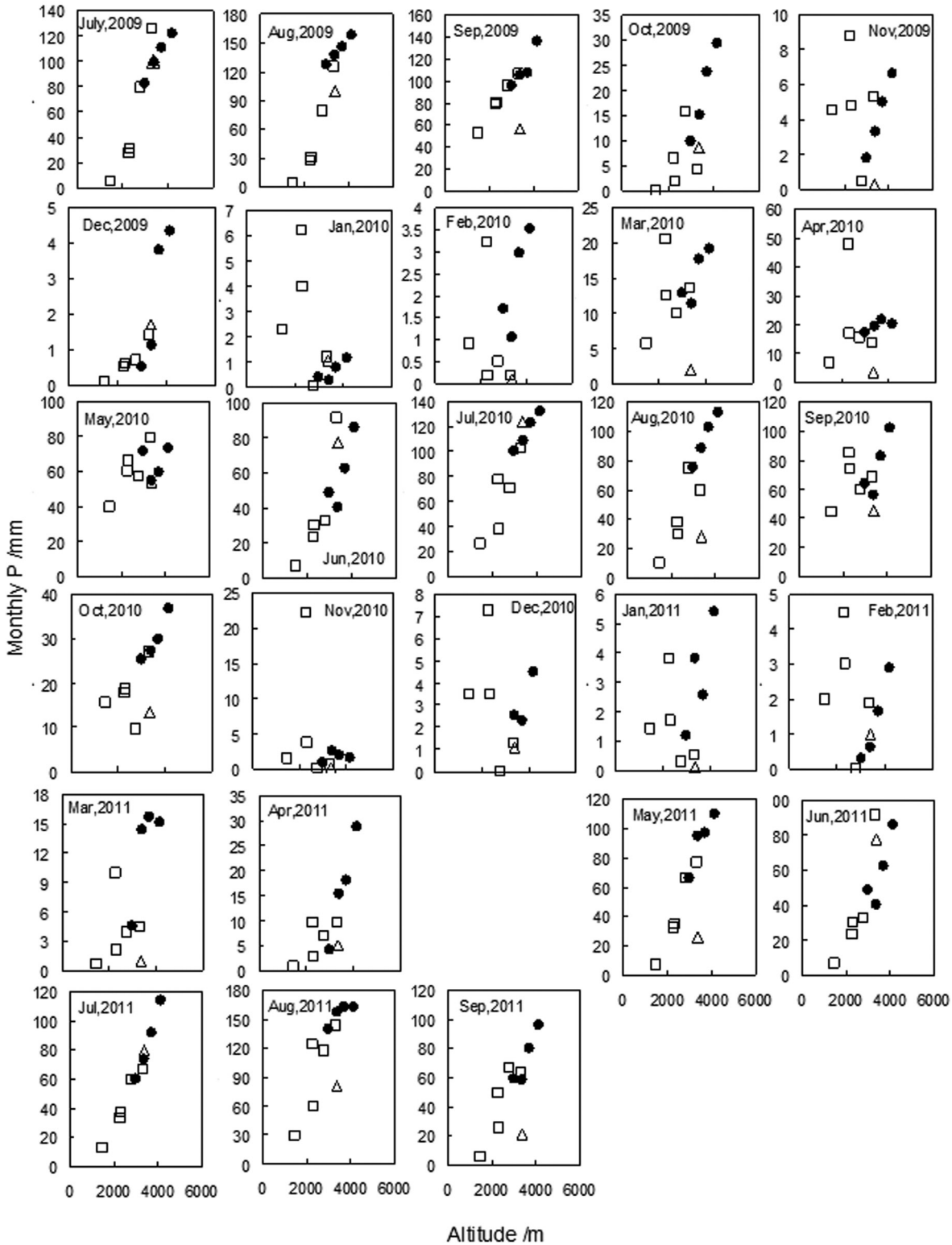

FIGURE 4. Monthly precipitation along altitude from July 2009 to September 2011 in the upstream section of the Heihe mainstream basin (dots, triangles, and squares represent data from the Hulu watershed, Tuole station, and other stations listed in Table 2, respectively).

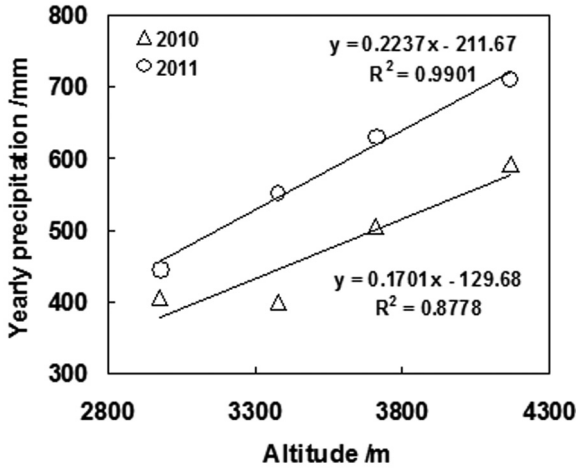

FIGURE 5. Precipitation gradients in the 2010 and 2011 hydrological years (from October to September) in the Hulu watershed.

seasons, probably because of the changeable climate in spring and autumn and little snowfall in winter (Fig. 4).

On a yearly scale, the gradient in the Hulu watershed is also different from one year to another, with an average value of about 200 mm km^{-1} (Fig. 5). In the 2010 hydrological year (from October 2009 to September 2010), the gradient was 170 mm km^{-1} (a = 0.01), while it was 223 mm km^{-1} in 2011 (a = 0.01).

Totalizer data are of relatively poor quality due to long measuring intervals and a lack of regular observation and maintenance, especially in the long cold winter. Both the totalizer and automatic station data collected in the Hulu watershed are combined into yearly P figures (Fig. 6). The 2011 data are better than those collected in 2010, with a gradient of about 204 mm km^{-1} (a = 0.05), close to that shown in Fig. 5.

Moreover, the so-called maximum P elevation zone is not found on a yearly scale in either the Hulu watershed (Figs. 5 and 6) or the upstream section of the Heihe mainstream watershed (Fig. 7). In Figure 7, the yearly P gradients are 193 and 210 mm km^{-1} with an equal R^2 value of 0.83 (a = 0.05) in the 2010 and 2011 hydrological years, respectively. These values are close to those observed in the Hulu small watershed.

Researchers have consistently observed orographic P in the Qilian Mountains for several decades, especially in recent years (e.g., Tang, 1985; Zhang et al., 2008; Wang et al., 2009a; Ding et al., 2009; Li et al., 2010; Liu et al., 2011). However, most of these results lack data from higher regions. Tang (1985) considers P across the Qilian Mountains as a whole and is of the opinion that the P-altitude relationship follows an S shape, meaning there should be two maximum P elevation zones. This is different from the pattern shown in Figure 7, though on a monthly scale, the S shape does appear in certain months (e.g., July 2010, August 2011; Fig. 4). Because of the inadequate nature of the data shown in Figure 7, the data shown in Figure 2 and Table 2 from six adjacent stations (1960–2011) in the Heihe River basin are used to provide a comparison with Tang's results. As shown in Figure 8, there is no S-shape relationship between P and altitude over the past 52 years. The data still follow a linear curve, with an average P gradient of 112 mm km^{-1} and a lower R^2 value of 0.57 (Fig. 8, part a, a = 0.10). The data distribution shown in Fig. 8, part a, for the six stations used is similar to that illustrated in Figure 7. Although the annual P gradient follows an increasing trend from 1960 to 2011, the increasing trend is not evident (Fig. 8, part b, a = 0.5). Ding et al. (2009) also reported a linear expression with an altitudinal gradient of 141 mm km^{-1} using data collected at 13 stations (the mountainous stations are the same as those considered here) from 1960 to 2006 across the whole of the Heihe River basin (from the lower desert to the Qilian Mountains). Wang et al. (2009a) use data gathered at six stations in the Heihe River basin (1960–2004) to find an altitudinal gradient of 170 mm km^{-1} (also a linear curve) but use data measured at only two stations (Qilian and Yeniugou) located in the Qilian Mountains. In the Qiyi Glacier watershed (97.5°E; 39.5°N, 4304–5158 m; Wang et al., 2010) in the western part of the Heihe River basin, Wang et al. (2009a) reported the altitude of the maximum P zone to be about 4700 m using short-term (26 November 2007 through 12 September 2008) data measured by 10 totalizers (3760–4900 m). Their results show an S-shape curve similar to that concluded by Tang (1985) but different from that represented in Figure 7 in the same elevation ranges.

Different results are derived from station numbers and positions with different water vapor sources. There are three main water vapor sources in the Qilian Mountains: from west to east, they are the westerly, plateau monsoon and East Asian monsoon sources (Zhang et al., 2008; Xu et al., 2010). The upstream section of the Heihe River basin is the region where the three circulations intersect, bringing a more complex P distribution. Zhang et al. (2008) have reported clear differences between P gradients in the eastern (370 mm km^{-1}), central (200 mm km^{-1}), and western (130 mm km^{-1}) parts of the Qilian Mountains using

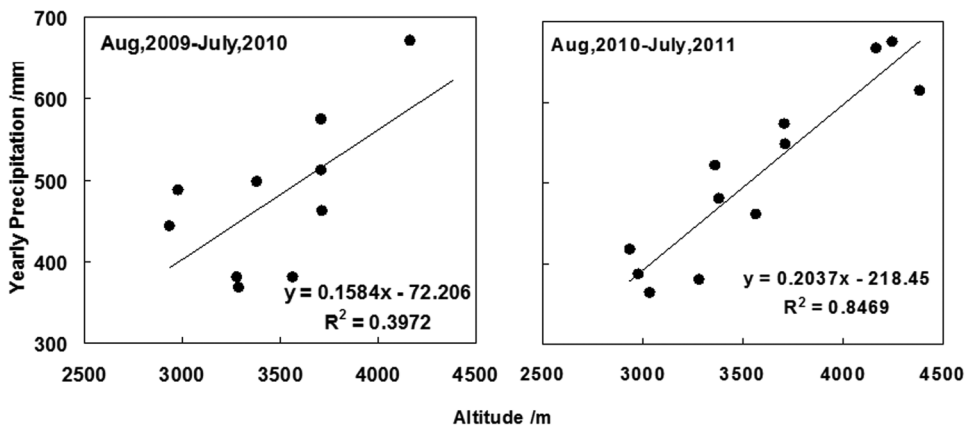

FIGURE 6. Precipitation gradients in 2010 and 2011 in the Hulu watershed (data from both totalizers and automatic stations).

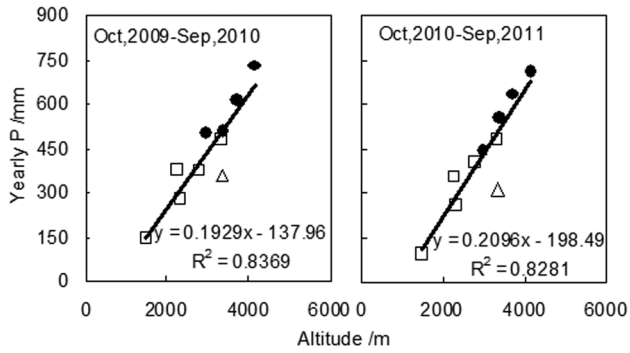

FIGURE 7. Yearly precipitation along altitude in the 2010 and 2011 hydrological years (from October to September) in the upstream section of the Heihe mainstream basin (dots, triangles, and squares represent data from the Hulu watershed, Tuole station, and other stations listed in Table 2, respectively).

pre-1993 data. Their P gradient for the central Qilian Mountains where the upstream section of the Heihe River basin lies is similar to that shown in Figure 7. Liu et al. (2011) also reported clear P gradient differences between the eastern (119 mm km^{-1}), central (46 mm km^{-1}), and western (8.7 mm km^{-1}) parts of the Qilian Mountains using Tropical Rainfall Measuring Mission (TRMM) and ground data, though the altitudinal gradient is much lower than the observed value due to coarse spatial resolution of TRMM data and other reasons. In sum, as Ward et al. (2011) have stated, in a complex mountain range like the Qilian Mountains, P data produced from space and at ground level are still not satisfactory. Establishing a P monitoring network in different parts of large alpine mountain ranges remains an urgent priority.

AIR TEMPERATURE (T)

On a large spatial scale, T varies negatively with altitude in warm seasons and latitude in cold seasons in China (Fang 1992; Chen et al., 2006). Weng and Sun (1984) have earlier analyzed the T lapse rate in China, while Fang (1988, 1992) reported the T lapse rate in different latitude groups across China using routine weather data gathered at lower elevations in both studies. In mountainous environments, spatiotemporal temperature patterns are particularly complex due to the existence of both regional and landscape-scale physiographic controls in these systems (Dobrowski et al., 2009), whereas T is arguably the single most important component of mountain climate (Barry, 1992). In our research on the small alpine watershed (Hulu; the data used here were gathered at a height of 1.5 m), T mainly varies with altitude, but in cold seasons this rule is somewhat undermined due to temperature inversion, such as in November 2009, November and December 2010, and January and February 2011 (Fig. 9).

Observed air temperature lapse rates show distinct spatial, seasonal, synoptic, and diurnal variations in alpine terrain (e.g., Richner and Phillips, 1984; Rolland, 2003; Minder et al., 2010; Prömmel et al., 2010; Lewkowicz and Bonnaventure, 2011; Kirchner et al., 2012). In recent years, the annual lapse rate commonly used is 5 or 6 °C km^{-1} (Bethan et al., 1996) with a climatological mean of 5.5 °C km^{-1} (Körner, 2007) based on extensive analysis of global climate records. In the Hulu watershed, the lapse rate of daily mean T varies greatly with unexpected strong temperature inverse samples (e.g., in winter 2010 and 2011, July 2010; Fig. 9, part a), and this also shows itself in the monthly mean lapse rates as reported in the literature. On a monthly scale, it is subject to seasonal variations similar to those of P, with values of about 4 to ~6.0 °C km^{-1} and 3 to ~ 4 °C km^{-1} in warm and cold seasons, respectively (Fig. 9, part b, a = 0.01). On a yearly scale (and also in hydrological years), lapse rates for the last two years are close to an average value of 4.8 °C km^{-1} (Fig. 10, a = 0.01), which is lower than the mean global value.

In the upstream section of the Heihe mainstream watershed, the linear relationship between T and altitude is well defined on a monthly scale other than in cold seasons (Fig. 11), and the mean yearly (2010 and 2011) T lapse rate is 4.8 °C km^{-1} (a = 0.01), close to that observed in the Hulu watershed (Fig. 12, parts a and b; a = 0.01). On a yearly scale, the lapse rate has been about 1 °C km^{-1} weaker at higher elevations (>3000 m) in recent years (Fig. 12, part c), indicating that the decreasing trend in the value of T with a rise in altitude diminishes at higher elevations. This finding is different from the results obtained in the Colorado Rocky Mountains (Pepin and Losleben, 2002).

Amplified warming at high elevations became apparent during the first half of the 20th century and has resulted in a general decrease in near-surface lapse rates (Price and Vaughan, 1993; Pepin and Losleben, 2002). Historical data from 1960 to 2011 (Table 2) for the upstream section of the Heihe mainstream river basin show an indistinct decreasing trend in annual (a = 0.4), warm (a = 0.1), and cold (a = 0.7) seasonal T lapse rates (Fig. 13). Similar to the results reported by Holden and Rose (2011) for uplands in the UK (though the climate is different), seasonal lapse rates in the upstream section of the Heihe mainstream river basin have also changed and become

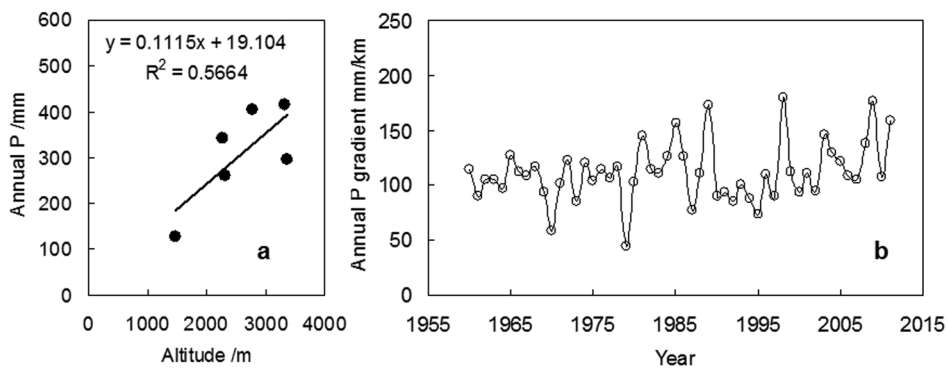

FIGURE 8. Annual P-altitude relationship in upstream regions below an elevation of 3400 m in the Heihe mainstream watershed. (a) Mean annual P from 1960 to 2011 varies with altitude; (b) annual P altitudinal gradient varies from 1960 to 2011.

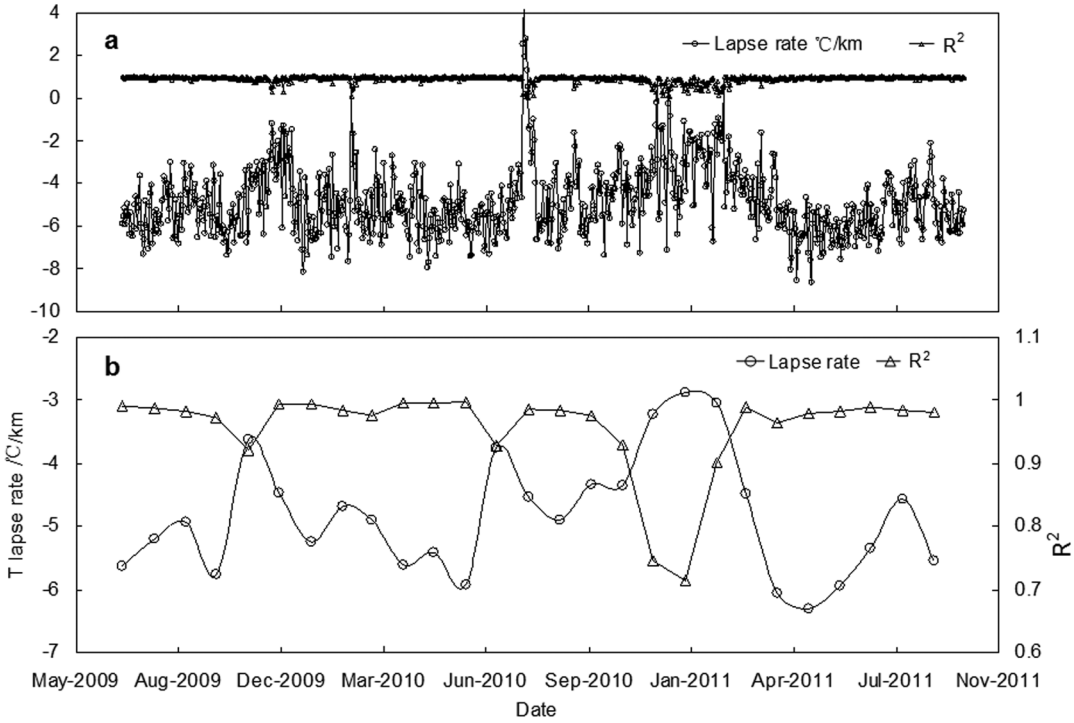

FIGURE 9. Lapse rate of (a) daily and (b) monthly average temperature (T) and its R^2 value from July 2009 to September 2011 in the Hulu watershed.

more divergent between winter and summer half-years (summer decreases more quickly), though the pattern is not obvious (Fig. 13).

In the upstream section of the Heihe mainstream river basin, the mean annual T lapse rate was about 5.6 °C km^{-1} from 1960 to 2011 (mean R^2 = 0.986, a = 0.01; data from 1483 to 3367 m), which is close to the mean global value (Körner, 2007). Zhang et al. (2001) obtain a lapse rate of 5.7 °C km^{-1} using data gathered at seven routine stations (forest regions, 1680–3045 m, from 1988 to 1998; R^2 = 0.94) in the eastern and central parts of the Qilian Mountains. Wang et al. (2009b) have reported a lapse rate of 5.1 °C km^{-1} (R^2 = 0.88) based on self-observed data gathered from seven stations (3200 to ~4300 m) on the southern slopes of the central Qilian Mountains in 2007. In other alpine regions, Xie et al. (2010) reported a value of 6.1 °C km^{-1} (R^2 = 0.97) using one year of data (August 2006–July 2007) from nine stations on the southern slopes (from 4300 to 5500 m; 91°02′E, 30°29′N) of the Nyainqentanglha Mountains south of the Tibetan Plateau. Other reports come from watersheds in several glaciers with short-term warm season data, such as those of Bai (1989; Glacier No. 1 at the headwaters of the Urumqi River, Tien Shan), Zhang and Yao (1993; the Guliya ice cap in the West Kunlun Mountains), Liu et al. (1996; Kangwure Glacier, Himalayas), and Han et al. (2008; Koxkar Glacier, Tien Shan). Their lapse rates range from 6.0 °C km^{-1} to 12.0 °C km^{-1}. Wang et al. (2011) calculated an average value of 4.8 °C km^{-1} across the whole Tibetan Plateau using data from 108 routine weather stations with elevations no higher than 4800 m. The above results show that the annual T lapse rate varies from 5 °C km^{-1} to 6 °C km^{-1} in different parts of China's cold alpine regions, the exception being glacier watersheds where data are limited. This range is similar to both the commonly used annual lapse rate of 5 °C km^{-1} or 6 °C km^{-1} (Bethan et al., 1996) and the climatological mean of 5.5 °C km^{-1} (Körner, 2007) based on extensive analysis of global climate records.

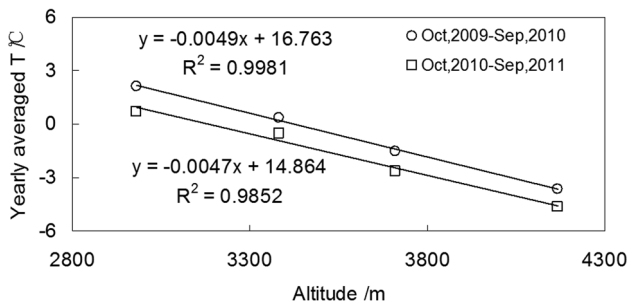

FIGURE 10. Lapse rate of annual (hydrological year) T in the Hulu watershed.

HUMIDITY AND WATER VAPOR PRESSURE

Monthly mean relative humidity (RH) in the Hulu watershed varied from 30% to 80% between July 2009 and September 2011 (Fig. 14, part a). Small RH differences are found among elevations varying from 2980 to 4166 m. In most months and on a yearly scale, the elevation zone between 3500 and 3700 m has the maximum RH value in both the Hulu watershed (Fig. 14, part b) and the upstream section of the Heihe mainstream watershed (Fig. 14, part c).

Monthly mean water vapor pressure (WVP) and absolute humidity (AH) have a well-defined altitudinal gradient (Fig. 15), though RH differs little across the four sites in the Hulu watershed. The WVP and AH lapse rates are subject to regular

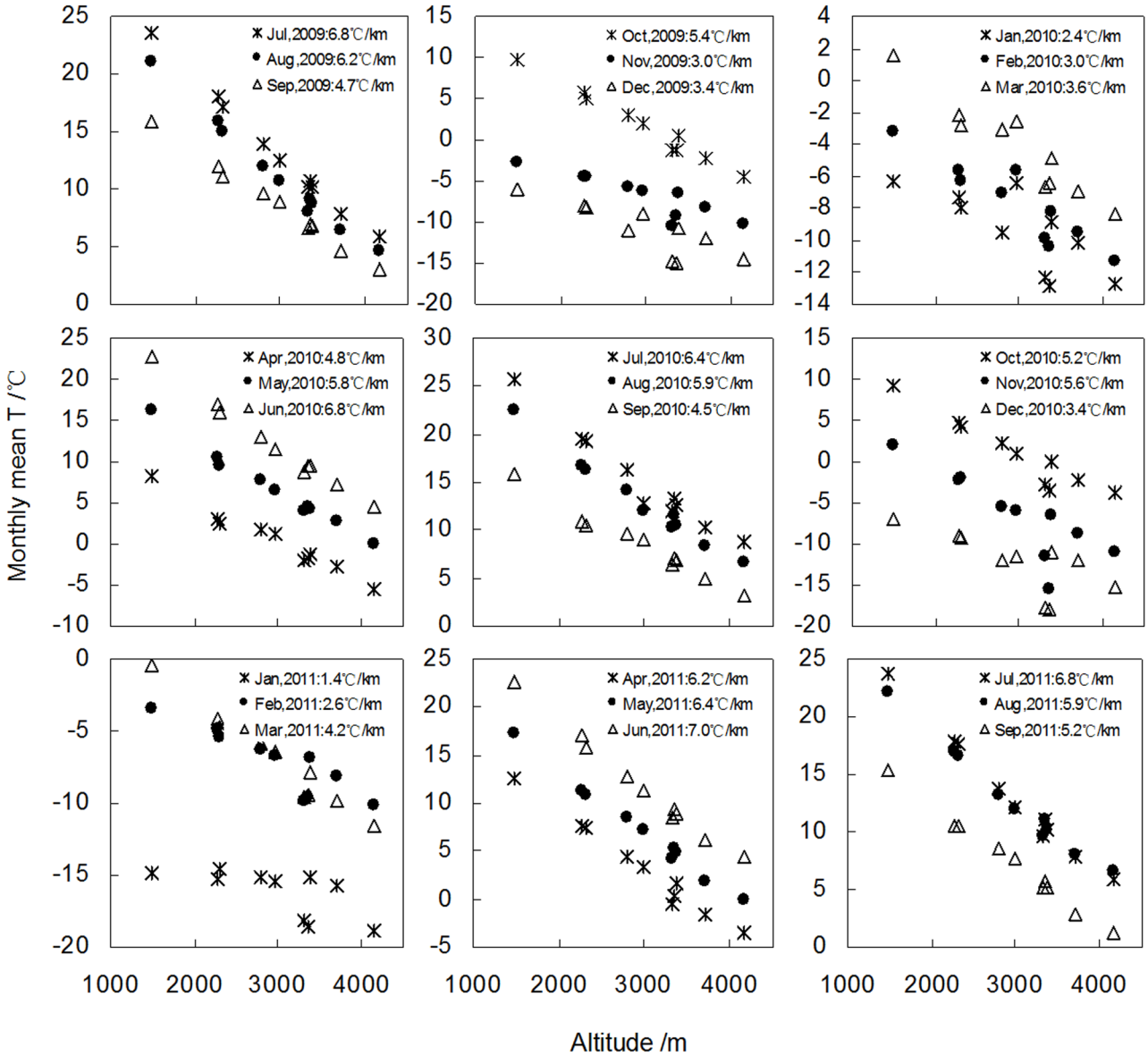

FIGURE 11. Monthly T along altitude from July 2009 to September 2011 in the upstream section of the Heihe mainstream basin (data from Hulu watershed and stations listed in Table 2).

seasonal variations, with larger values occurring in warm seasons. The yearly mean WVP and AH lapse rates (for the 2010 and 2011 hydrological years) are about 1.1 hpa km^{-1} (R^2 = 0.969, a = 0.01) and 0.84 g m^{-3} km^{-1} (R^2 = 0.959, a = 0.01), respectively.

SOLAR RADIATION AND SOIL SURFACE TEMPERATURE (TS)

Near surface global radiation (G) is mainly controlled by position (latitude and longitude), cloud (sunshine hours), topography (shadowing), and the clearness index (Chen et al.,

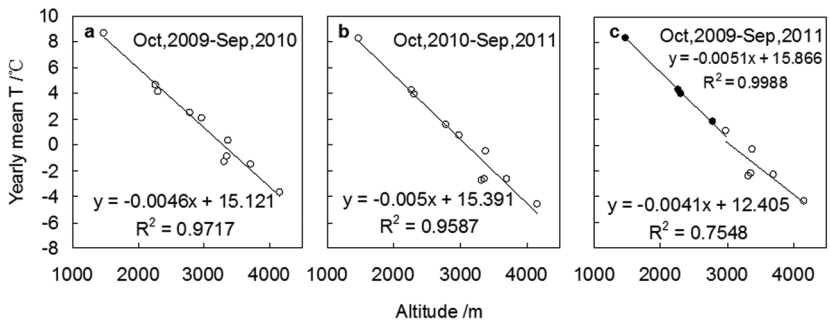

FIGURE 12. Yearly T lapse rate (hydrological year) in the upstream section of the Heihe mainstream basin (data from Hulu watershed and stations listed in Table 2).

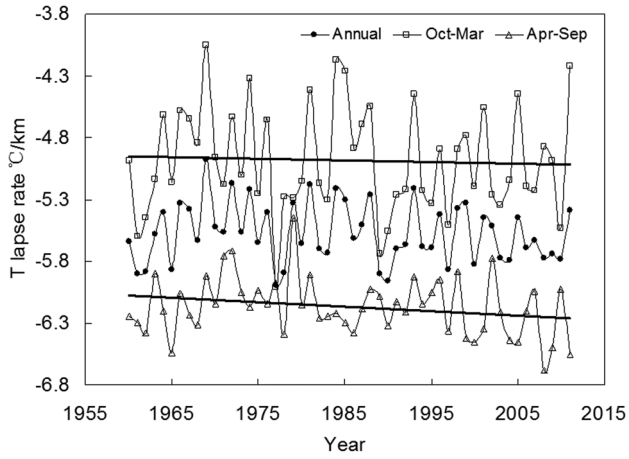

FIGURE 13. Annual, cold, and warm seasonal T lapse rate varies from 1960 to 2011 in the upstream section of the Heihe mainstream basin (data from stations listed in Table 2).

2007). In warm seasons, except in some large-scale rainy days, the altitudinal gradient appears, meaning changeable weather (more cloud and convectional rain) causes lower G readings at higher elevations in the Hulu watershed (Fig. 16, part a). Because the fixed stations are not far away and their shadowing are less in the warm seasons, their G should be close on the clear days, and the only cause of lower G readings at higher elevations is the appearance of cloud. In cold seasons, the large-scale weather situation dominates. Thus, G gradient found little between lower and higher regions in snowy months (March and April), while in other cold months, too evident G gradient appears mainly because of topographic shadowing at sites no. 2 and 3 (Tables 1 and 3, Fig. 16, part b). Because of topography limits, site no. 2 lies 500 m behind a mountain peak and is shaded in about December and January, while site no. 3 lies at a highland in a valley with shading from November to January. This shading would decrease the measured air temperature T to some extent. From this point of view, the reported yearly TLR in part Air Temperature (T) (also the winter ones) should be less than the 4.8 °C km^{-1}.

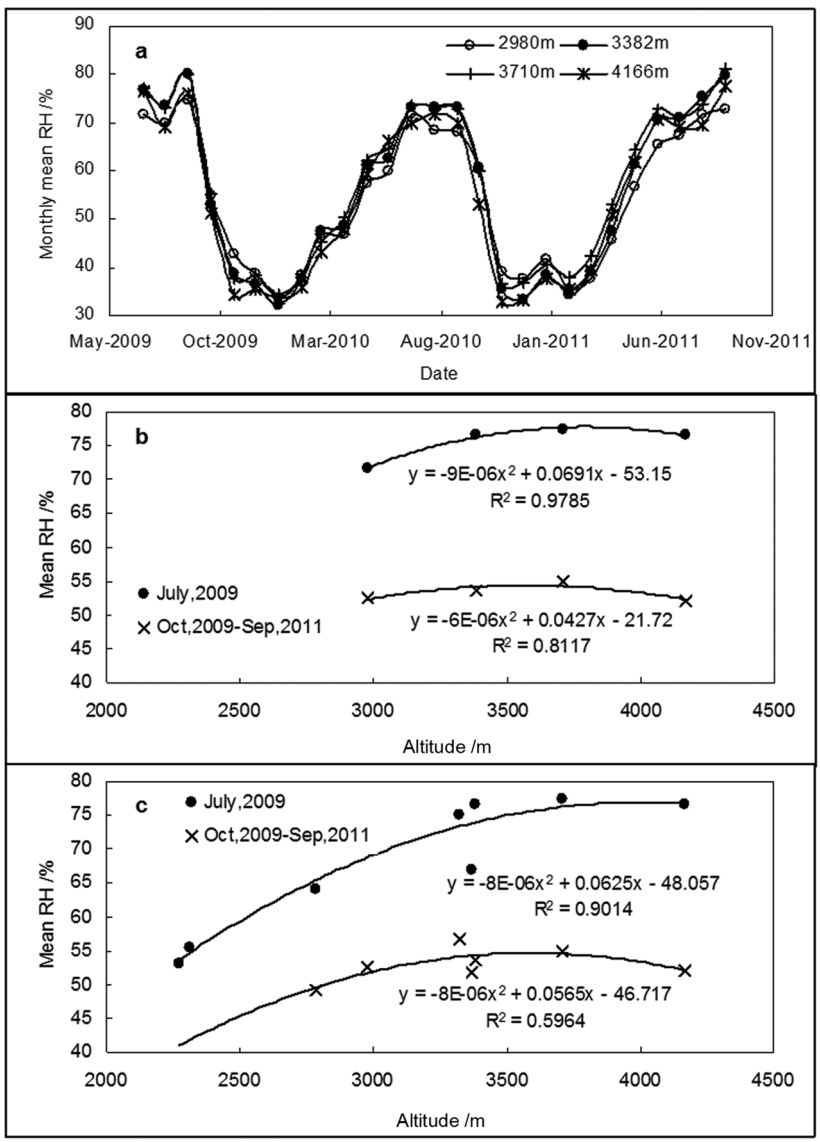

FIGURE 14. Spatial and temporal variation of relative humidity (RH) in Hulu watershed and upstream section of Heihe mainstream watershed. (a) Monthly mean RH from July 2009 to September 2011 in Hulu watershed; (b) monthly and yearly mean RH varies along altitude in Hulu watershed; (c) monthly and yearly mean RH varies along altitude in upstream section of Heihe mainstream watershed.

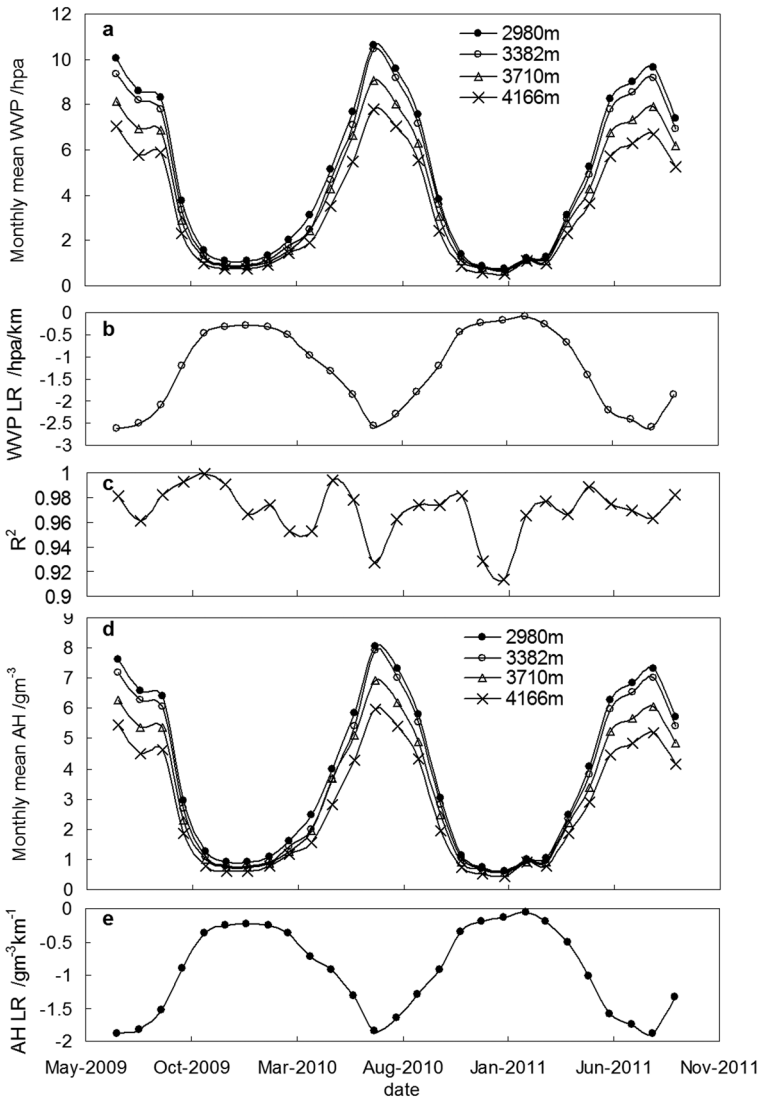

FIGURE 15. Monthly mean water vapor pressure (WVP) and absolute humidity (AH) and their lapse rate (LR) variations from July 2009 to September 2011 in the Hulu watershed. (a) Monthly mean WVP; (b) lapse rate of WVP; (c) R^2 value of the linear relationship between WVP and altitude; (d) monthly mean AH; (e) lapse rate of AH.

In most months and on a yearly scale, the albedo of marshy meadow (site no. 2, Table 3) is the largest, especially in cold seasons when ice forms and snow lies on the ground for a long period due to shadowing (Fig. 16, part c). In the vegetation growing season (June–September), the albedo is little affected by cryosphere, with mean values of 0.25 and 0.17 in meadow and alpine desert areas, respectively. The long-term existence of snow cover increases the albedo significantly across the whole Hulu watershed in most months. Thus, mean albedo on an annual basis is larger, with values of about 0.22, 0.30, 0.35, and 0.27 at sites no. 5, 1, 2, and 3, respectively.

The highest level of net radiation flux (N) is found at site no. 1 (the lowest area), with only minor differences being detected at other sites, though the altitudinal gradient appears in most months (Fig. 16, part d). In addition to net short-wave radiation, one of the key factors affecting N is the soil surface temperature (Ts) based on the Stefan-Boltzman law (Stefan, 1879), largely according to land use type. Monthly mean Ts in the Hulu watershed has an evident lapse rate, with an average R^2 value of 0.779 and a mean lapse rate of 7.5 °C km^{-1} from July 2009 to September 2011 (a = 0.05). Ts at sites no. 2 and 3 (Tables 1 and 3) is similar (Fig. 16, part e), though there is a large altitude difference (456 m) between them. This is likely to be explained by the low soil water content and low vegetation cover at site no. 3. Abnormal Ts variations appear in some cold months (e.g., winter 2010; Fig. 16, part e) at site no. 2 (marshy meadow), mainly because of the formation of ice with high albedo (Fig. 16, part c) and freezing latent heat.

Despite the effects of net short-wave radiation and air temperature T (downward long-wave radiation; Campbell, 1985), there is a well-defined linear relationship between monthly mean N and Ts (Fig. 17, a = 0.01).

Summary

This paper gives an overview of a cryosphere-hydrology observation system recently established in the Hulu small alpine watershed in the Qilian Mountains of northwest China. Meteorology, glaciers, frozen soil, snow, and basic water balance items in areas of alpine desert, alpine meadow, forest, alpine shrubs, and alpine grassland, as well as groundwater, have been monitored since August 2008. The altitudinal gradients of major weather factors in the small watershed are analyzed and discussed on both monthly and yearly scales.

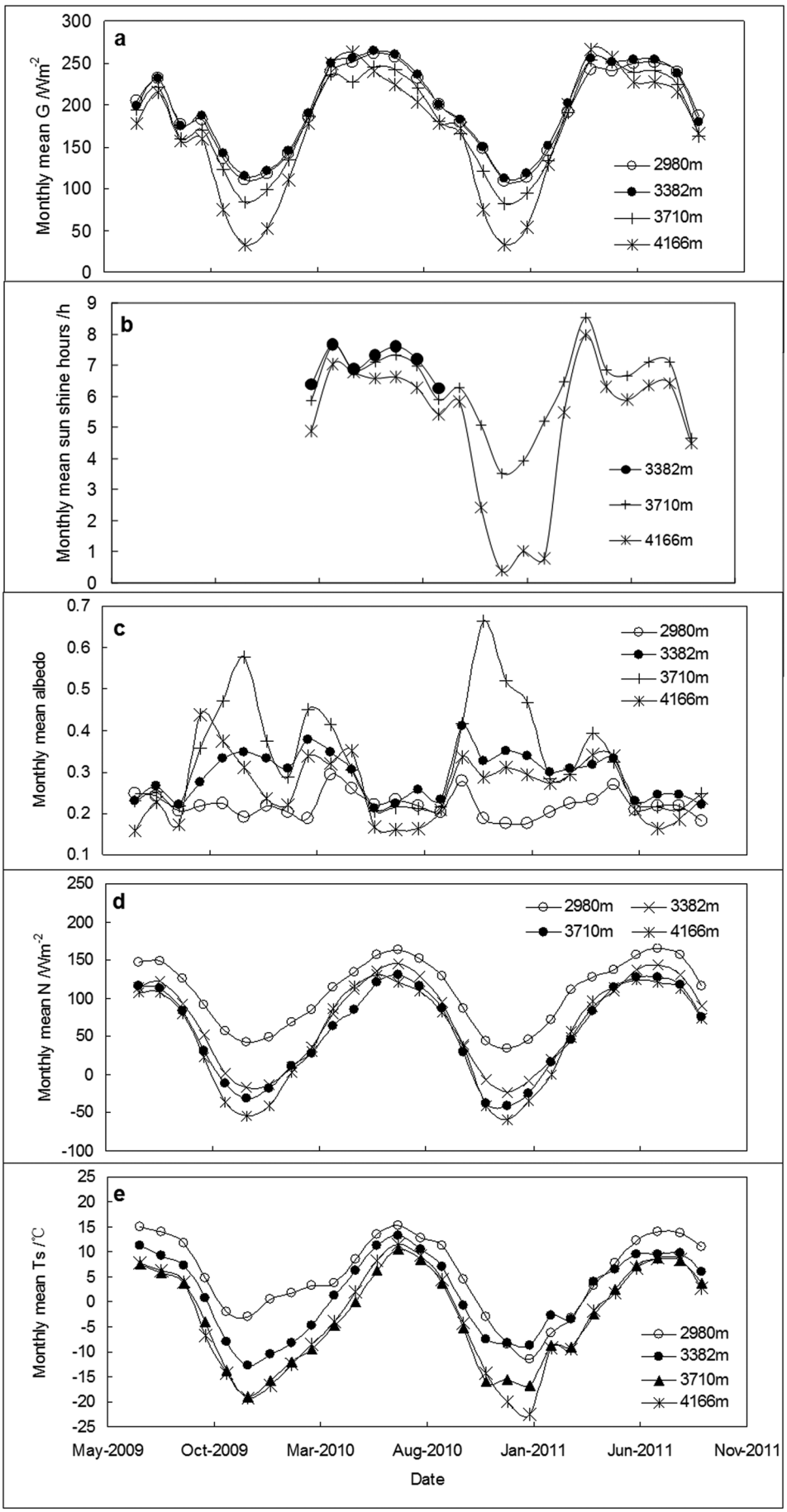

FIGURE 16. Monthly mean solar radiation and soil surface temperature from July 2009 to September 2011 in the Hulu watershed. (a) Global radiation; (b) sunshine hours; (c) albedo; (d) net radiation; (e) soil surface temperature.

TABLE 3

Underlying surfaces of the four automatic stations used.

Station No.	Land use	Main vegetation	Coverage (%)	Max. height (cm)	Superficial soil
1	Alpine meadow	*Kobresia humilis*	100	30	Loam
2	Marshy meadow	*Kobresia humilis*	85	10	Clay
3	Alpine desert		0	0	Gravel
5	Alpine grassland	*Kobresia humilis; Carex moorcroftii* Falc. ex Boott*; Stipa purpurea* Griseb.	100	50	Loam

(1) Although the monthly precipitation (P) gradient displays clear seasonality, good linear relationships between yearly P and altitude are found to have operated in the 2010 and 2011 hydrologic years (200 mm km^{-1}) in both the Hulu watershed (data from 2980 to 4166/4248 m) and the upstream section of the Heihe mainstream basin (data from 1483 to 4166 m) where the Hulu watershed is located. Similar phenomena also appear to have occurred from 1960 to 2011 in regions below an elevation of 3367 m in the upstream section of the Heihe mainstream, where the P gradient has increased marginally over the past 52 years. However, due to the effects of three water vapor flows (westerly, plateau monsoon, and East Asian monsoon) on the upstream section of the Heihe and the complexity of orographic P in large alpine mountains, more P monitoring networks are still needed.

(2) The air temperature (T) lapse rate and variations therein are evident on daily, monthly, and yearly scales in both the Hulu watershed and the upstream section of the Heihe mainstream basin, other than when temperature inversion occurs. The yearly T lapse rate has been about 1 °C km^{-1} weaker at higher elevations (>3000 m) in the past 2 years. Indistinct decreasing trends in annual, warm, and cold seasonal T lapse rates occurred from 1960 to 2011 in the upstream section of the Heihe, where seasonal lapse rates become more divergent between winter and summer half-years. Data presented here (a mean annual T lapse rate of about 5.6 °C km^{-1} from 1960 to 2011 with a mean R^2 of 0.99) and in other reports show the annual T lapse rate varies between 5 °C km^{-1} and 6 °C km^{-1} in China's cold regions, a rate close to the mean global value.

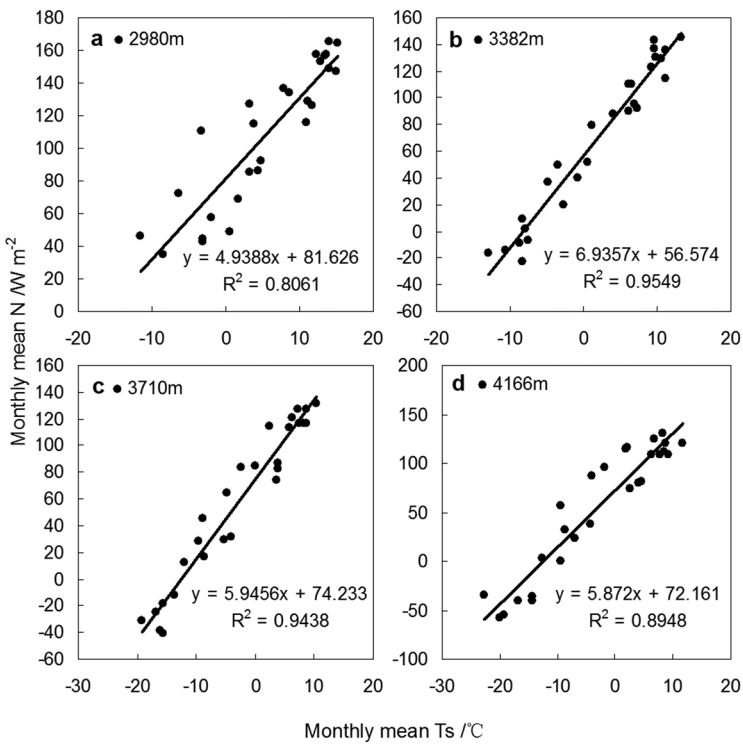

FIGURE 17. Relationship between monthly mean N and Ts in the Hulu watershed.

(3) The elevation zone between 3500 and 3700 m has the maximum relative humidity (RH) value in the upstream section of the Heihe. The lapse rates for monthly mean water vapor pressure (WVP) and absolute humidity (AH) are subject to regular seasonal variations, with larger values occurring in warm seasons and yearly means of 1.1 hpa km^{-1} (R^2 = 0.97) and 0.84 g m^{-3} km^{-1} (R^2 = 0.96), respectively.

(4) The long-term existence of snow cover increases the albedo, with yearly values of 0.22, 0.30, 0.35, and 0.27 in areas of grassland, meadow, marshy meadow, and alpine desert, respectively. The highest net radiation flux (N) is found in lower grasslands with small differences being detected at other sites, though the effect of altitude appears in most months. A well-defined linear relationship between monthly mean N and soil surface temperature (Ts) is found to operate in the Hulu watershed according to land use type, while Ts has a mean lapse rate of 7.5 °C km^{-1} with an average R^2 value of 0.78 from July 2009 to September 2011.

In the next one or two years, the local precipitation calibration methods using wind and DFIR data, the half-empirical surface temperature formula for snow melting and soil heat transferring processes, and the glacier and snow runoff model including snowdrift and energy balance will be given. At the same time, the water and heat balance on six typical alpine underlying surfaces and their hydrological functions could be published. A distributed hydrological model named HULU for Chinese alpine regions is in design based on the measurements in Hulu watershed.

Acknowledgment

This paper is principally supported by the National Natural Sciences Foundation of China (grant numbers 91025011, 41222001, 91125013, and 91025001).

References Cited

Ahrens, B., 2006: Distance in spatial interpolation of daily rain gauge data. *Hydrology & Earth System Sci*ences, 10: 197–208, doi: http://dx.doi.org/10.5194/hess-10-197-2006.

Aizen, V. B., Aizen, E. M., and Melack, J. M., 1996: Precipitation, melt and runoff in the northern Tien Shan. *Journal of Hydrology*, 186: 229–251.

Akkiraz, M. S., Akgün, F., Utescher, T., Bruch, A. A., and Mosbrugger, V., 2011: Precipitation gradients during the Miocene in western and central Turkey as quantified from pollen data. *Palaeogeography, Palaeoclimatology, Palaeoecology*, 304: 276–290, doi: http://dx.doi.org/10.1016/j.palaeo.2010.05.002.

Bai, C., 1989: Study on the relationship between glacier and climate. *Journal of Glaciology and Geocryology*, 11(4): 287–297 (in Chinese).

Barry, R. G., 1992: *Mountain Weather and Climate*. London: Routledge, 412 pp.

Barry, R. G., 2008: *Mountain Weather and Climate.* Cambridge: Cambridge University Press, 413 pp.

Basist, A., Bell, G. D., and Meentemeyer, V., 1994: Statistical relationships between topography and precipitation patterns. *Journal of Climate,* 7: 1305–1315.

Bethan, S., Vaughan, G., and Reid, S. J., 1996: A comparison of ozone and thermal tropopause height and the impact of tropopause definition of quantifying the ozone content of the troposphere. *Quarterly Journal of the Royal Meteorological Society*, 122: 929–944.

Campbell, G. S., 1985: *Soil Physics with BASIC: Transport Models for Soil-Plant Systems*. Amsterdam: Elsevier, 150 pp.

Chen, R., and Han, C., 2010: Hydrology, ecology and climate significance and its research progress of the alpine cold desert. *Advance in Earth Science*, 25(3): 255–263 (in Chinese).

Chen, R., Kang, E., Zhang, Z., Zhao, W., Song, K., Zhang, J., and Lan, Y., 2004: Estimation of tree transpiration and response of tree conductance to meteorological variables in desert-oasis system of northwest China. *Science in China Series D Earth Sciences*, 47(Suppl. 1): 9–20, doi: http://dx.doi.org/10.1360/04zd0002.

Chen, R., Kang, E., Ji, X., Yang, J., and Yang, Y., 2006: Cold regions in China. *Cold Regions Science and Technology*, 45: 95–102. doi: http://dx.doi.org/10.1016/j.coldregions.2006.03.001.

Chen, R., Kang, E., Ji, X., Yang, J., and Wang, J., 2007: An hourly solar radiation model under actual weather and terrain conditions: a case study in Heihe River basin. *Energy,* 32: 1148–1157. doi: http://dx.doi.org/10.1016/j.energy.2006.07.006.

Chen, R., Lu, S., Kang, E., Ji, X., Zhang, Z., Yang, Y., and Qing, W., 2008: A distributed water-heat coupled model for mountainous watershed of an inland river basin in Northwest China (I): model structure and equations. *Environmental Geology*, 53: 1299–1309, doi: http://dx.doi.org/10.1007/s00254-007-0738-2.

Ding, R., Wang, F., Wang, J., and Liang, J., 2009: Analysis on spatial-temporal characteristics of precipitation in Heihe River basin and forecast evaluation in recent 47 years. *Journal of Desert Research*, 29(2): 335–341 (in Chinese).

Dobrowski, S. Z., Abatzoglou, J. T., Greenberg, J. A., and Schladowet, S. G., 2009: How much influence does landscape-scale physiography have on air temperature in a mountain environment? *Agricultural and Forest Meteorology*, 149: 1751–1758, doi: http://dx.doi.org/10.1016/j.agrformet.2009.06.006.

Fang, J. Y., 1988: Climate and vegetation in China (I). Changes in the altitudinal lapse rate of temperature and distribution of sea level temperature. *Ecological Research,* 3: 37–51.

Fang, J. Y., 1992: Studies on geographic distribution of the altitudinal lapse rate of temperature in China. *Chinese Science Bulletin*, 37: 1979–1983.

Fo, B. P., 1992: The effects of topography and elevation on precipitation. *Acta Geographica Sinica,* 47(4): 303–314 (in Chinese).

Goodison, B. E., Louie, P. Y. T., and Yang, D., 1998: WMO solid precipitation measurement intercomparison. World Meteorological Organization, final report WMO/TD-No.872.

Han, H., Liu, S., Ding, Y., Xiao, D., Wang, Q., Xie, C., Wang, J., Zhang, Y., and Li, J., 2008: Near-surface meteorological characteristics on the Koxkar Baxi Glacier. Tianshan, *Journal of Glaciology and Geocryology,* 30(6): 965–975 (in Chinese).

Holden, J. and Rose, R., 2011: Temperature and surface lapse rate change: a study of the UK's longest upland instrumental record. *International Journal of Climatology,* 31: 907–919, doi: http://dx.doi.org/10.1002/joc.2136.

Johnson, G. L., and Hanson, C. L., 1995: Topographic and atmospheric influences on precipitation variability over a mountainous watershed. *Journal of Applied Meteorology,* 34: 68–87.

Kang, E., Cheng, G., Song, K., Jin, B., Liu, X., and Wang, J., 2005: Simulation of energy and water balance in Soil-Vegetation-Atmosphere Transfer system in the mountain area of Heihe River basin at Hexi Corridor of northwest China. *Science in China Series D Earth Sciences,* 48(4): 538–548, doi: http://dx.doi.org/10.1360/02yd0428.

Kang, E., Chen, R., Zhang, Z., Ji, X., and Jin, B., 2008: Some scientific problems facing research on hydrological processes in an inland river basin. *Frontiers of Earth Science in China,* 2(4): 384–392, doi: http://dx.doi.org/10.1007/s11707-008-0050-9.

Kirchner, M., Faus-Kessler, T., Jakobi, G., Leuchner, M., Ries, L., Scheel, H.-E., and Suppan, P., 2012: Altitudinal temperature lapse rates in an Alpine valley: trends and the influence of season and

weather patterns. *International Journal of Climatology*, 33: 539–555, doi: http://dx.doi.org/10.1002/joc.3444.

Körner, C., 2007: The use of 'altitude' in ecological research. *Trends in Ecology and Evolution*, 22: 569–574, doi: http://dx.doi.org/10.1016/j.tree.2007.09.006.

Kotlarski, S., Bosshard, T., Lüthi, D., Pall, P., and Schär, C., 2012: Elevation gradients of European climate change in the regional climate model COSMO-CLM. *Climatic Change*, 112: 189–215, doi: http://dx.doi.org/10.1007/s10584-011-0195-5.

Lauscher, F., 1976: Weltweite typen der hohenabhangigkeit des niederschlags. *Wetter und Leben*, 28: 80–90.

Lewkowicz, A. G., and Bonnaventure, P. P., 2011: Equivalent elevation: a new method to incorporate variable lapse rates into mountain permafrost modeling. *Permafrost and Periglacial Processes*, 22: 153–162, doi: http://dx.doi.org/10.1002/ppp.720.

Li, X., Li, X., Li, Z., Ma, M., Wang, J., Xiao, Q., Liu, Q., Che, T., Chen, E., Yan, G., Hu, Z., Zhang, L., Chu, R., Su, P., Liu, Q., Liu, S., Wang, J., Niu, Z., Chen, Y., Jin, R., Wang, W., Ran, Y., Jin, X., and Ren, H., 2009: Watershed allied telemetry experimental research. *Journal of Geophysical Research*, 114: D22103, doi: http://dx.doi.org/10.1029/2008JD011590.

Li, Y., Zhang, Q., Xu, X., and Ma, Y., 2010: Relationship between precipitation and terrain over the Qilian Mountains and their ambient areas. *Journal of Glaciology and Geocryology,* 32(1): 52–61, http://en.cnki.com.cn/Article_en/CJFDTOTAL-BCDT201001008.htm (in Chinese).

Lin, Z., 1995: *Climatology of Orographic Precipitation*. Beijing: Science Press, 126 pp. (in Chinese).

Liu, J., Chen, R., Qing, W., and Yang, Y., 2011: Study on the vertical distribution of precipitation in mountainous regions using TRMM data. *Advance in Water Sciences*, 22(4): 447–454.

Liu, S., Xie, Z., and Ma, L., 1996: Characteristics of summer climate in area of Kangwure Glacier, Mt. Xixiabangma. *Journal of Glaciology and Geocryology*, 18(3): 244–251.

Marquínez, J., Lastra, J., and García, P., 2003: Estimation models for precipitation in mountainous regions: the use of GIS and multivariate analysis. *Journal of Hydrology*, 270: 1–11, doi: http://dx.doi.org/10.1016/S0022-1694(02)00110-5.

Michaelides, S., Levizzani, V., Anagnostou, E., Bauer, P., Kasparis, T., and Lane, J. E., 2009: Precipitation: measurement, remote sensing, climatology and modeling. *Atmospheric Research*, 94: 512–533, doi: ttp://dx.doi.org/10.1016/j.atmosres.2009.08.017.

Minder, J. R., Mote, P. W., and Lundquist, J. D., 2010: Surface temperature lapse rates over complex terrain: lessons from the Cascade Mountains. *Journal of Geophysical Research*, 115: D14122, doi: http://dx.doi.org/10.1029/2009JD013493.

Nuttall, M., and Callaghan, T. V., 2000: *The Arctic: Environment, People, Policy*. Amsterdam: Harwood Academic Publishers, 245 pp.

Pepin, N., and Losleben, M., 2002: Climate change in the Colorado Rocky Mountains: free air versus surface temperature trends. *International Journal of Climatology*, 22: 311–319.

Prat, O. P., and Barros, A. P., 2010: Ground observations to characterize the spatial gradients and vertical structure of orographic precipitation—Experiments in the inner region of the Great Smoky Mountains. *Journal of Hydrology*, 391: 141–156, doi: http://dx.doi.org/10.1016/j.jhydrol.2010.07.013.

Price, J. D., and Vaughan, G., 1993: The potential for stratosphere-troposphere exchange in cut-off-low systems. *Quarterly Journal of the Royal Meteorological Society*, 119: 343–365.

Prigent, C., 2010: Precipitation retrieval from space: an overview. *Comptes Rendus Geoscience*, 342: 380–389, doi: http://dx.doi.org/10.1016/j.crte.2010.01.004.

Prömmel, K, Geyer, B., Jones, J. M., and Widmann, M., 2010: Evaluation of the skill and added value of a reanalysis driven regional simulation for Alpine temperature. *International Journal of Climatology*, 30: 760–773, doi: http://dx.doi.org/10.1002/joc.1916.

Putkonen, J. K., 2004: Continuous snow and rain data at 500 to 4400 m altitude near Annapurna, Nepal, 1999–2001. *Arctic, Antarctic, and Alpine Research*, 36(2): 244–248, doi: http://dx.doi.org/10.1657/1523-0430(2004)036[0244:CSARDA]2.0.CO;2.

Richner, H., and Phillips, P. D., 1984: A comparison of temperature from mountaintops and the free atmosphere—Their diurnal variation and mean difference. *Monthly Weather Review*, 112(7): 1328–1340.

Rizzi, R., Bauer, P., Crewell, S., Leroy, M., Mätzler, C., Menzel, W. P., Ritter, B., Russell, J. E., and Thoss, A., 2006: Cloud, precipitation and large scale land surface imaging (CPL) observational requirements for meteorology, hydrology, and climate. Position paper, version 3. Available from http://eumeds.eumetsat.int/groups/pps/documents/document/pdf_peps_pp_cloud_prec_land.pdf.

Roe, G. H., 2005: Orographic precipitation. *Annual Review of Earth and Planetary Sciences*, 33: 645–671, doi: http://dx.doi.org/10.1146/annurev.earth.33.092203.122541.

Rolland, C., 2003: Spatial and seasonal variations of air temperature lapse rates in Alpine regions. *Journal of Climate*, 16: 1032–1046, doi: http://dx.doi.org/10.1175/1520-0442(2003)016<1032:SASVOA>2.0.CO;2.

Rubel, F., and Rudolf, B., 2001: Global daily precipitation estimates proved over the European Alps. *Meteorologische Zeitschrift*, *N.F.*, 10: 403–414.

Sevruk, B., and Mieglitz, K., 2002: The effect of topography, season and weather situation on daily precipitation gradients in 60 Swiss valleys. *Water Science and Technology*, 45: 41–48.

Sevruk, B., and Nevenic, M., 1998: The geography and topography effects on the areal pattern of precipitation in a small prealpine basin. *Water Science and Technology*, 37: 163–170.

Shen, Z., 1975: Characteristics of precipitation in Mount Qomolangma. *In* Xizang Science Expedition Team of the Chinese Academy of Sciences (eds.), *Scientific Report of the Investigation on Mt Qomolangma (1966–1968), Meteorology and Solar Radiation*. Beijing: Science Press, 11–20 (in Chinese).

Stefan, J., 1879: Über die Beziehung zwischen der Wärmestrahlung und der Temperatur. *In* Sitzungsberichte der mathematisch-naturwissenschaftlichen Classe der kaiserlichen Akademie der Wissenschaften, Bd. 79 (Wien 1879), S. 391–428.

Tang, M. C., 1985: The distribution of precipitation in mountain Qilian (Nanshan). *Acta Geographica Sinica*, 40(4): 323–332 (in Chinese).

Thomas, A., 1997: The climate of the Gongga Shan Range, Sichuan Province, PR China. *Arctic and Alpine Research*, 29(2): 226–232.

Wang, Z., 1981: Glacier inventory of China (I) Qilian Mountains. Lanzhou: Lanzhou Institute of Glaciology and Cryopedology, Academia Sinica (in Chinese), 135 pp.

Wang, N., He, J., Jiang, X., Song, G., Pu, J., Wu, X., and Chen, L., 2009a: Study on the zone of maximum precipitation in the north slopes of the central Qilian Mountains. *Journal of Glaciology and Geocryology*, 31(3): 395–403, http://en.cnki.com.cn/Article_en/CJFDTotal-BCDT200903000.htm (in Chinese).

Wang, J., Li, Y., Du, M., Wang, Q., Tang, Y., Xue, X., Zhang, F., and Wang, S., 2009b: The features of microclimate and vegetation distribution on the southern Lenglongling, Qilian Mountains. *Journal of Mountain Science*, 27(4): 418–426 (in Chinese).

Wang, N., He, J., Pu, J., Xi, J., and Jing, Z., 2010: Variations in equilibrium line altitude of the Qiyi Glacier, Qilian Mountains, over the past 50 years, *Chinese Science Bulletin*, 55: 3810–3817, doi: http://dx.doi.org/10.1007/s11434-010-4167-3.

Wang, K., Sun, J., Cheng, G., and Jiang, H., 2011: Effect of altitude and latitude on surface air temperature across the Qinghai-Tibet Plateau. *Journal of Mountain Science*, 8: 808–816, doi: http://dx.doi.org/10.1007/s11629-011-1090-2.

Ward, E., Buytaert, W., Peaver, L., and Wheater, H., 2011: Evaluation of precipitation products over complex mountainous terrain: a water resources perspective. *Advances in Water Resources*, 34: 1222–1231, doi: http://dx.doi.org/10.1016/j.advwatres.2011.05.007.

Weng, D., and Sun, Z., 1984: A preliminary study of the lapse rate of surface air temperature over mountainous regions of China. *Geographical Research*, 3(2): 24–34 (in Chinese).

Woo, M. K., 2008: *Cold region Atmospheric and Hydrologic Studies: the Mackenzie GEWEX Experience. Volume 1: Atmospheric Dynamics*. Berlin, Heidelberg: Springer-Verlag, 481 pp.

Wulf, H., Bookhagen, B., and Scherler, D., 2010: Seasonal precipitation gradients and their impact on fluvial sediment flux in the Northwest Himalaya. *Geomorphology*, 118: 13–21, doi: http://dx.doi.org/10.1016/j.geomorph.2009.12.003.

Xie, J., Liu, J., Du, M., and Wang, Z., 2010: Altitudinal distribution of air temperature over a southern slope of Nyainqentanglha Mountains, Tibetan Plateau. *Scientia Geographica Sinica*, 30(1): 113–118 (in Chinese).

Xu, J, Wang, K., Jiang, H., Li, Z., Sun, J., Luo, X., and Zhu, Q., 2010: A numerical simulation of the effects of Westerly and Monsoon on precipitation in the Heihe River basin. *Journal of Glaciology and Geocryology*, 32(3): 489–496 (in Chinese).

Zhang, X., and Yao, T., 1993: Preliminary analyses on the synoptic and climatic features in Guliya Ice Cap region. *Journal of Glaciology and Geocryology*, 15(3): 460–466 (in Chinese).

Zhang, H., Wen, Y., Ma, L., Chang, Z., and Wang, J., 2001: The climate features and regionalization of vertical climatic zones in the northern slope of Qilian Mountains. *Journal of Mountain Science*, 19(6): 497–502 (in Chinese).

Zhang, Q., Yu, Y., and Zhang, J., 2008: Characteristics of water cycle in the Qilian Mountains and the oases in Hexi inland river basins. *Journal of Glaciology and Geocryology*, 30(6): 907–913 (in Chinese).

MS accepted September 2013